Ionospheric Conductivity Dependence of Subauroral Polarization Streams (SAPS) Observed by the SuperDARN Hokkaido East HF Radar

Y. Zhang, N. Nishitani, and T. Hori (ISEE, Nagoya University)

Contents

Introduction

Motivation & Purpose

Data analysis

Standard model & Chisham model

Results

Conclusions & Future work

What is SAPS?

SAPS (SubAuroral Polarization Stream) defined as relatively narrow channel of enhanced westward flow, is caused by strong electric fields oriented poleward in the ionosphere, and is located equatorward of the auroral oval (subauroral region).

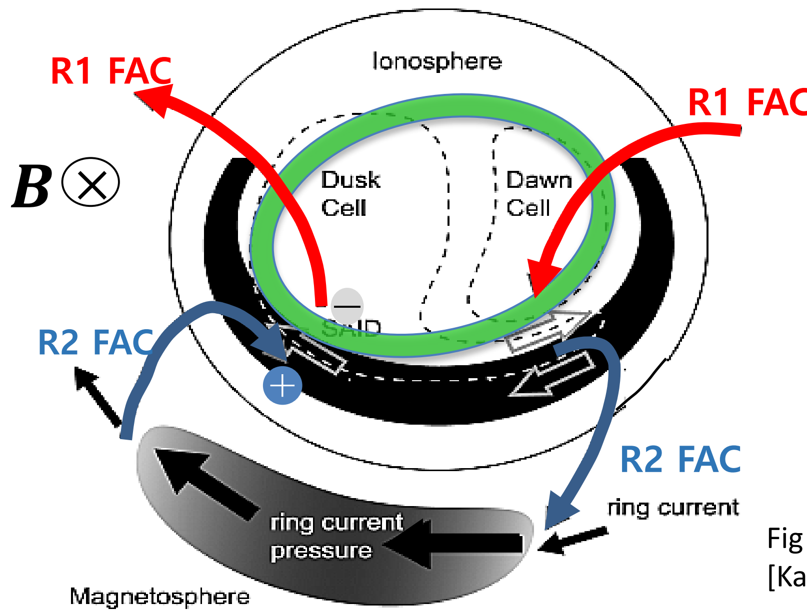

Fig 1. The generation of SAPS [Kataoka et al., 2007].

- Mostly occur during magnetically disturbed periods [Huang and Foster, 2007].
- Mlat. of the SAPS flow channels decreases linearly with both Dst and MLT [Foster and Vo, 2002].

Previous study

- There is a good correlation between the flux tube–integrated Pedersen conductivity due to solar illumination and the magnitude of the SAPS velocity [Wang et al., 2008].

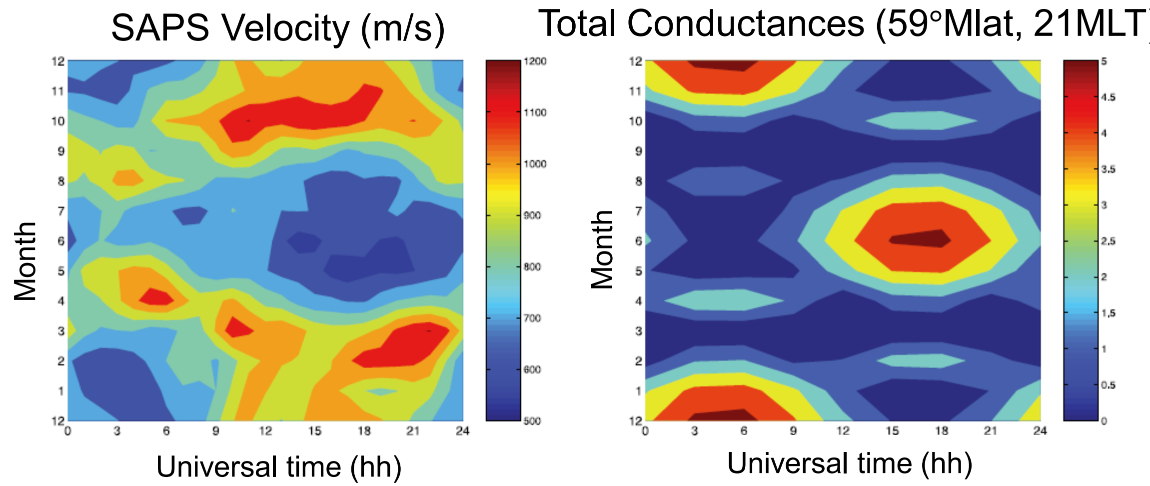

- SAPS tend to occur more poleward for larger flux tube–integrated conductivity [Wang et al., 2008].

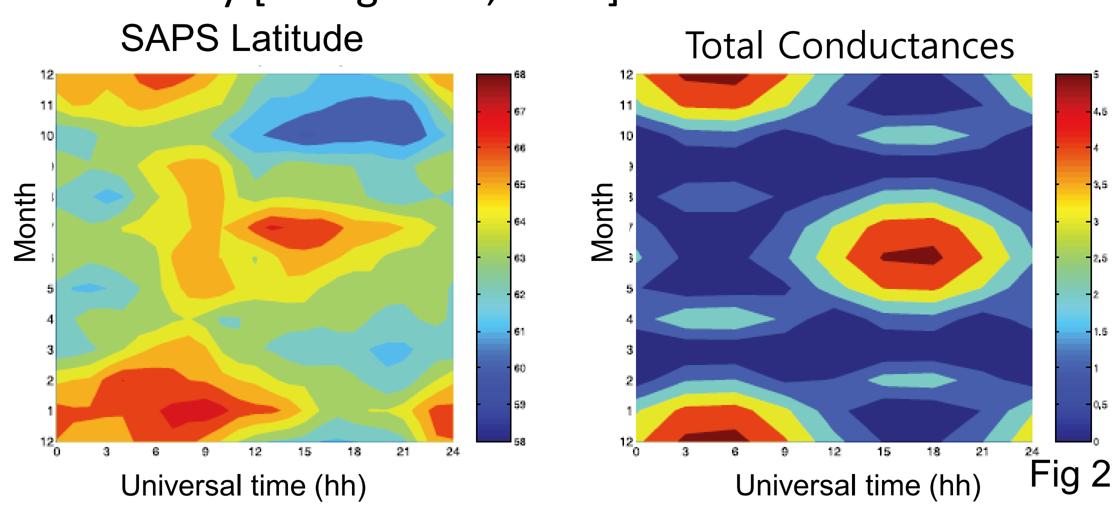

Fig 2. [Wang et al., 2008]

Motivation & Purpose

- Most of the previous studies mainly reported the characteristics and morphologies of SAPS. However, the occurrence of SAPS in response to solar illumination has so far not been fully investigated.

- To understand the mechanism and the characteristics of SAPS in more detail, it is necessary to investigate the influence of solar illumination upon SAPS.

↓

Using SuperDARN Hokkaido East Radar to study the influence of solar illumination upon SAPS

Instruments & Data set

■ Instruments

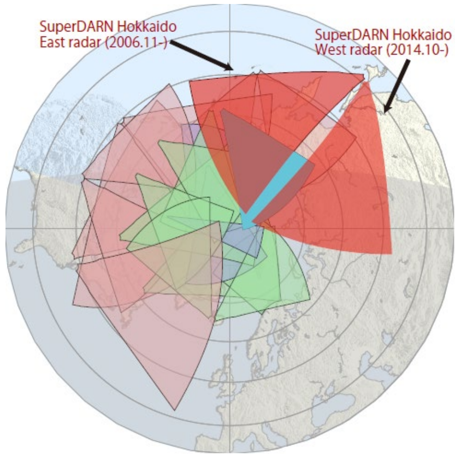

Fig 3. Field of view of the SuperDARN radar network.

- **SuperDARN Hokkaido East radar**
  Location: +43.53°, +143.61° (geographic coordinates)
  Time resolution: 1s ~ 2 min
  Space resolution: 15 km ~ 100 km
  Beam width: 5 degrees
- **NOAA POES Satellite**
  To define the location of auroral oval.

■ Data set

Total over 3180 days

Date	Time period
2008/01/10 to 2016/12/31	0300 ~ 0900 UT (12 ~ 18 LT)

60 events × 3 points = 180 data points

An example of SAPS event

LOS velocity obtained from SuperDARN

Auroral oval

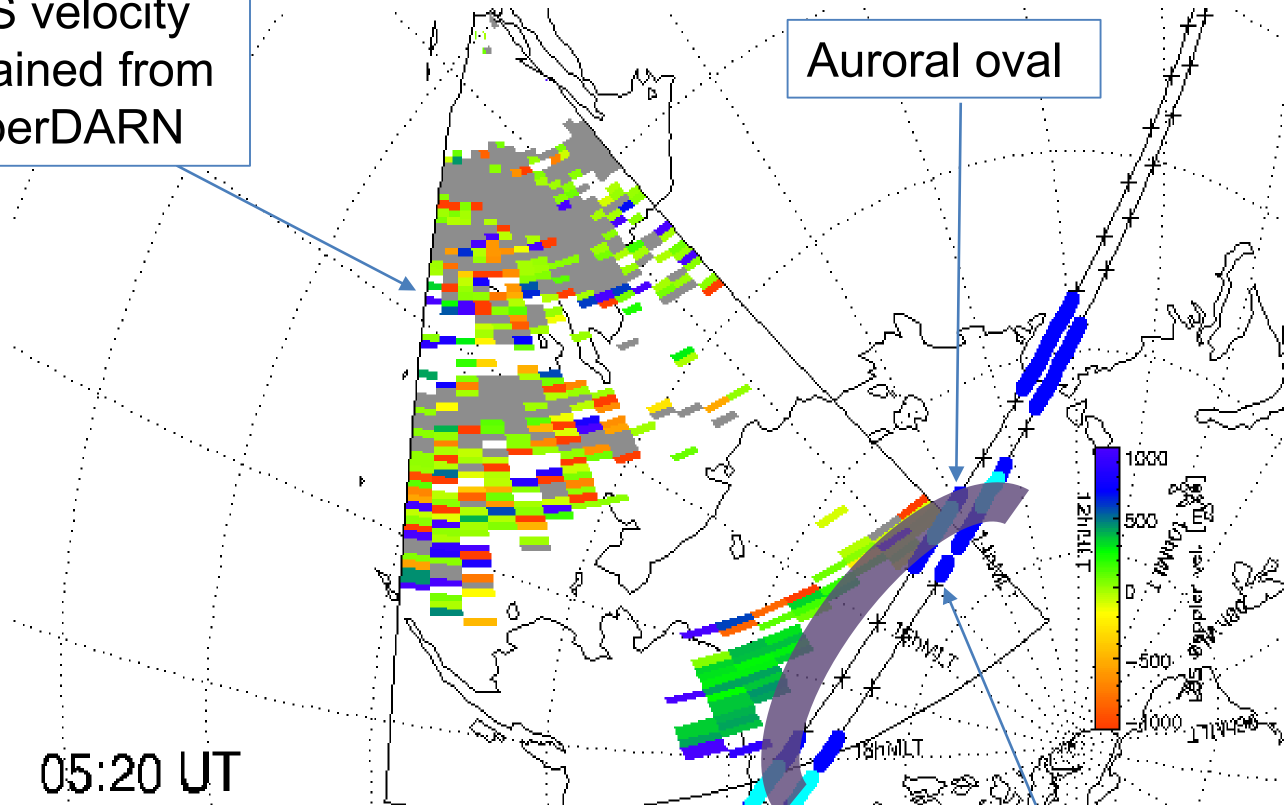

Fig 4. Example on December 15, 2012.

Precipitation energy flux obtained along the satellite's footprint

- Cyan color : flux > 1 mW/m^2
- Blue color : 0.1 < flux <1 (mW/m^2)

Introduction
Motivation & Purpose
Data analysis
Standard model & Chisham model
Results
Conclusions & Future work

Standard model (Commonly used)

Standard model:

- Assume a straight line virtual propagation path.
- Assume that the real and virtual propagation paths have approximately the same ground range.

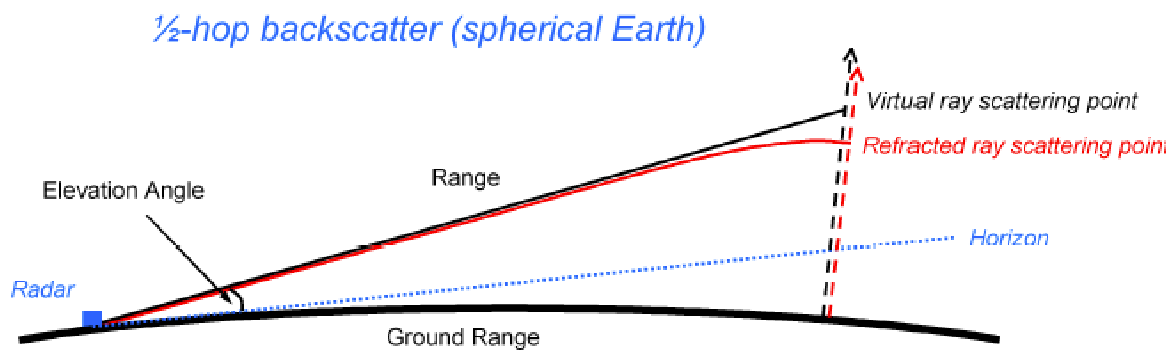

Fig 6. Schematic diagram illustrating refracted and virtual HF propagation paths for 1 ½-hop ionospheric backscatter assuming a spherical earth [Chisham et al., 2008].

$$h_v = \begin{cases} \frac{115r}{150} & \text{for } 0 < r < 150\,\text{km} \\ 115 & \text{for } 150 \le r \le 600\,\text{km} \\ \frac{r-600}{200}(h_i - 115) + 115 & \text{for } 600 < r < 800\,\text{km} \\ h_i & \text{for } r \ge 800\,\text{km} \end{cases}$$

The error in standard model could be larger than 60 km for 1½-hop F-region backscatter.

Introduction

Motivation & Purpose

Data analysis

Standard model & Chisham model

Results

Conclusions & Future work

Standard model & Chisham model

Pseudo virtual height:
The virtual height one needs to assume for 1½ hop backscatter in order to retain the correct ground range when using a ½ hop backscatter assumption.

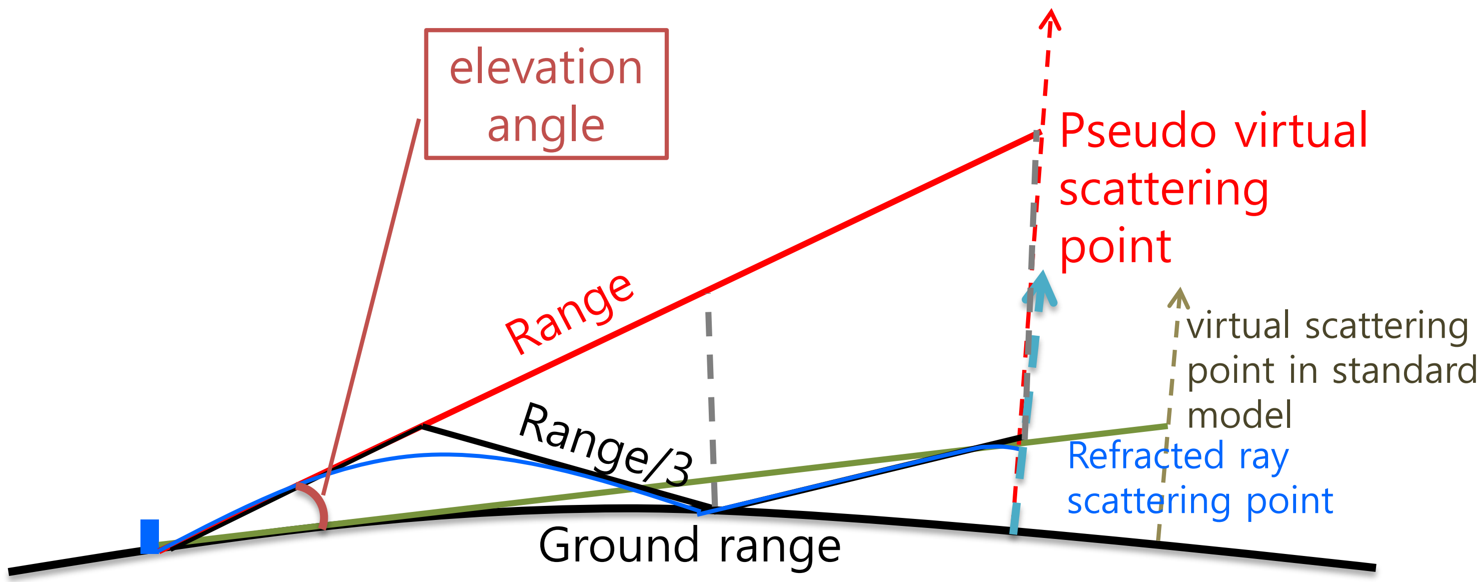

Fig 7. A simple schematic diagram illustrating the concept of pseudo virtual height for 1½ -hop backscatter. Modified from [Chisham et al., 2008].

Chisham model

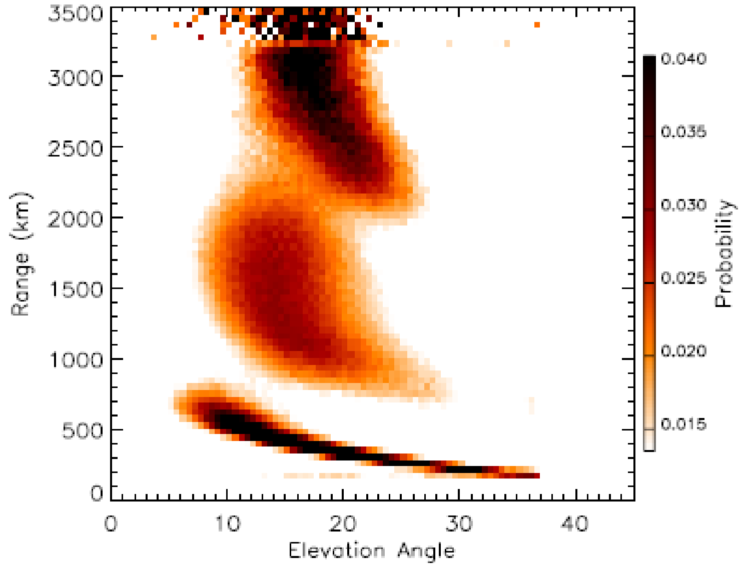

Fig 8. The distribution of ionospheric backscatters in range-elevation angle[Chisham et al., 2008].

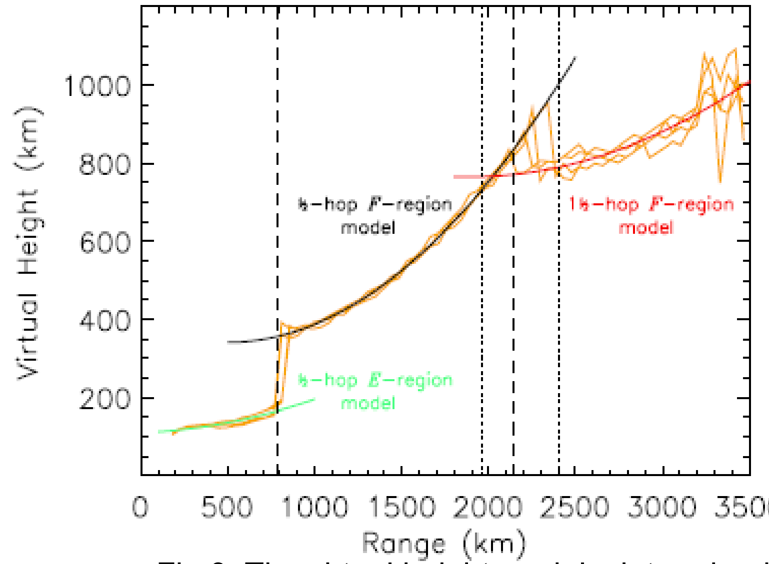

Fig 9. The virtual height models determined from the data set of the Saskatoon radar [Chisham et al., 2008].

Categorized backscatters into different propagation on the basis on the empirically obtained range-elevation angle relation

→

Calculates the pseudo virtual height of each range using different model corresponding to the backscatter's region.

→

Calculates the ground range of the backscatter based on pseudo virtual height .

Introduction

Motivation & Purpose

Data analysis

Standard model & Chisham model

Results

Conclusions & Future work

Distribution of elevation angle and range data from Hokkaido East Radar

Data set: Ionospheric echoes from all beams in 2013 – 2014.

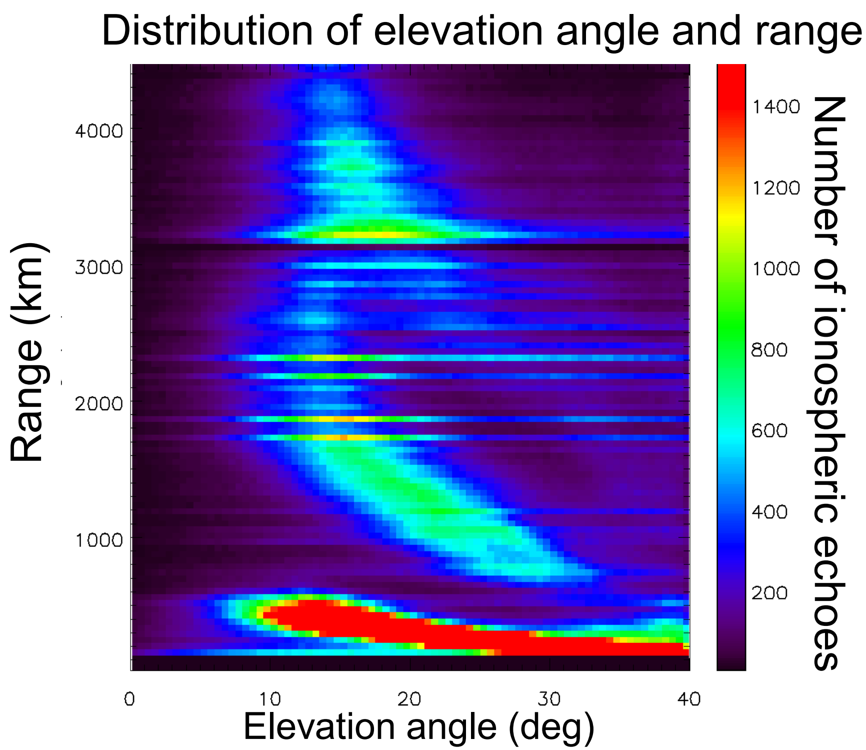

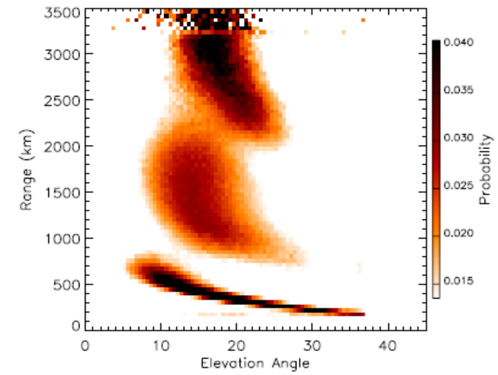

- Three distinct patterns of ionospheric backscatters are shown on the left.

Fig 10. The distribution of ionospheric backscatters in range-elevation angle.

Table 1. Different propagation path and its corresponding range of Hokkaido East radar.

Propagation path & Region	Range (km)
½ -hop E-region	- 650
½ -hop F-region	651 – 2900
1½ -hop F-region	2901 - 4300

Chisham model for Hokkaido East radar

- We obtained three separate models by fitting three low-order polynomial of the form

$$h(r) = A + Br + Cr^2$$

h: Virtual height r: Range

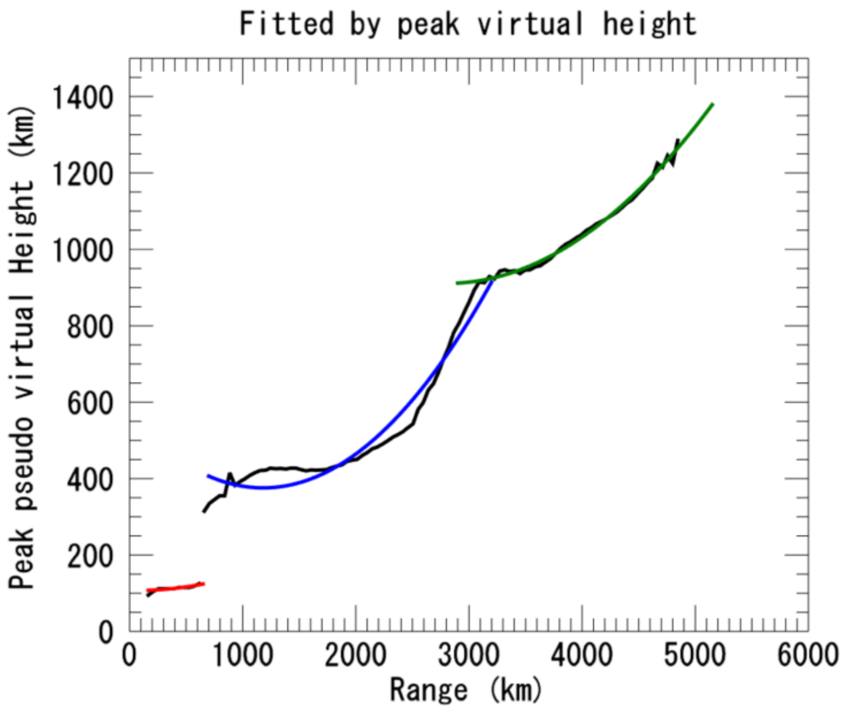

Fig 11. The virtual height models determined from the data set of the Hokkaido east radar.

Table 2. The coefficients for the three different virtual height models.

Backscatter Type	A	B	C
½ -hop E-region	107.398	-0.006634	4.98816×10^{-5}
½ -hop F-region	560.401	-0.312578	1.32294×10^{-4}
1½ -hop F-region	1580.36	-0.477314	8.50828×10^{-5}

Comparison of Chisham model & standard model for Hokkaido radar

Error=Standard model – Chisham model

- The error in high latitude F-region could be larger than 1.5° and 13° in latitude and longitude respectively.

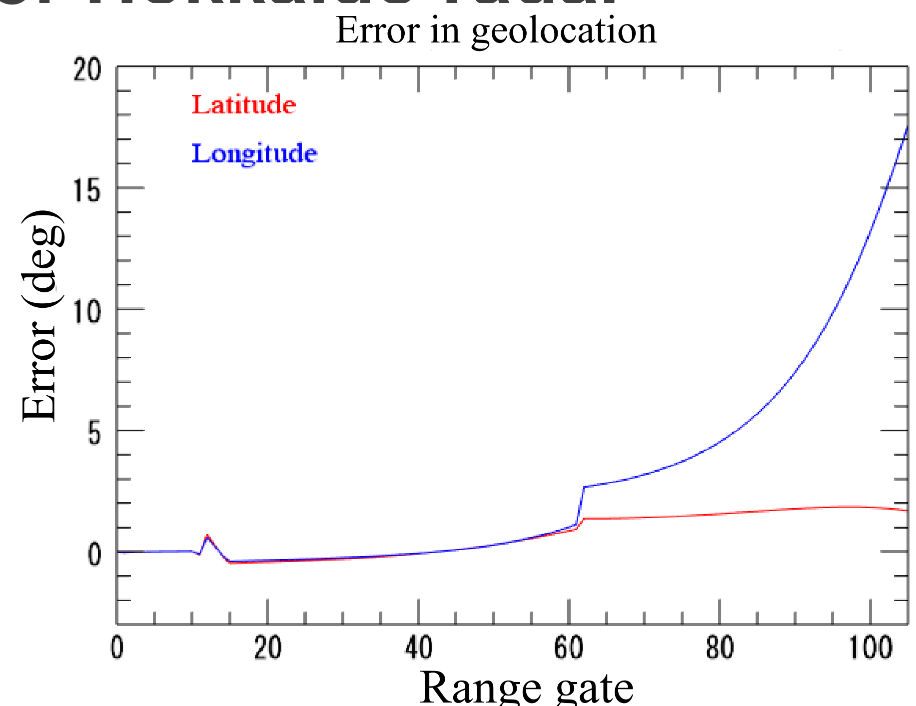

Fig 12. The virtual height models determined from the data set of the Hokkaido east radar.

Table 3. Error estimation.

Range (km)	Error in geolocation (+ means equatorward and westward)
2250	（0.282°，0.274°）
3600	（1.564°，4.520°）
4500	（1.828°，13.193°）

SZA calculated from Chisham model

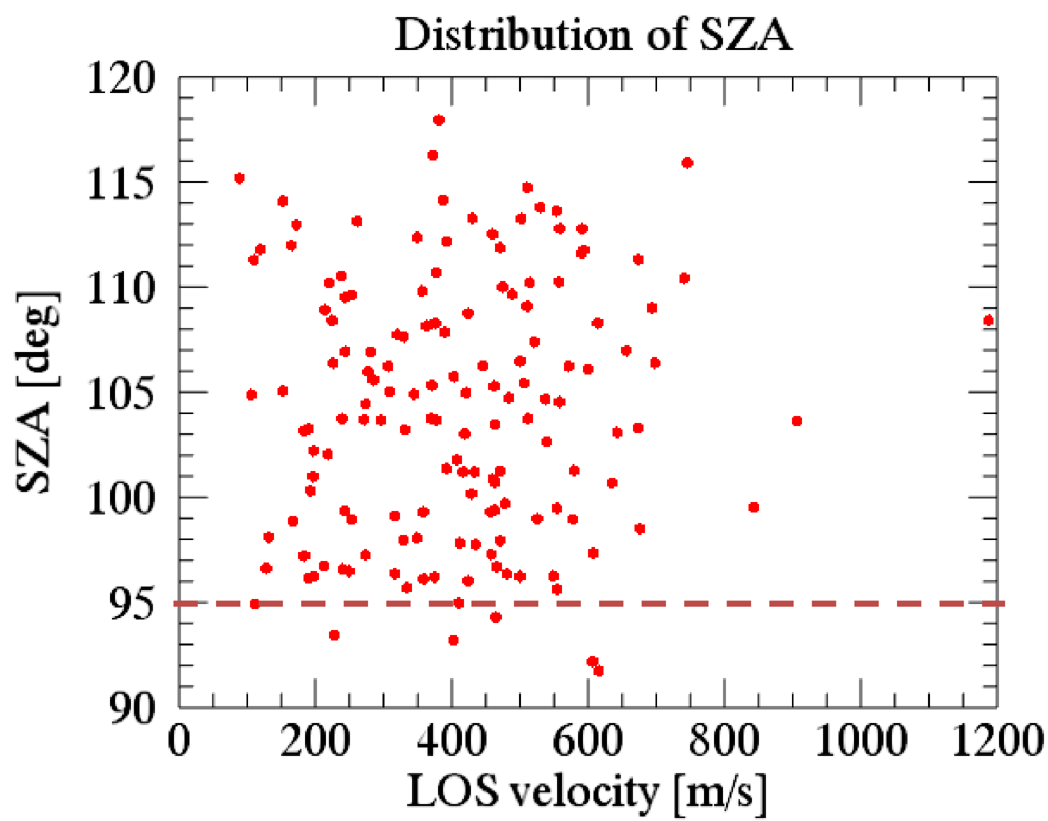

Fig 13. The distribution of SZA derived from the geolocation calculated by Chisham model. The red dash line shows the threshold of SZA of 95 degrees .

The threshold of SZA derived from Chisham model is 95 degrees.

LOS velocity and Westward velocity

- We converted the LOS velocity to westward velocity with L-shell fitting, which assumes that the flows are in magnetic longitude direction, then the true velocity can be expressed in the flowing form.

$$V_{LOS} = V_{true} \cos\theta$$

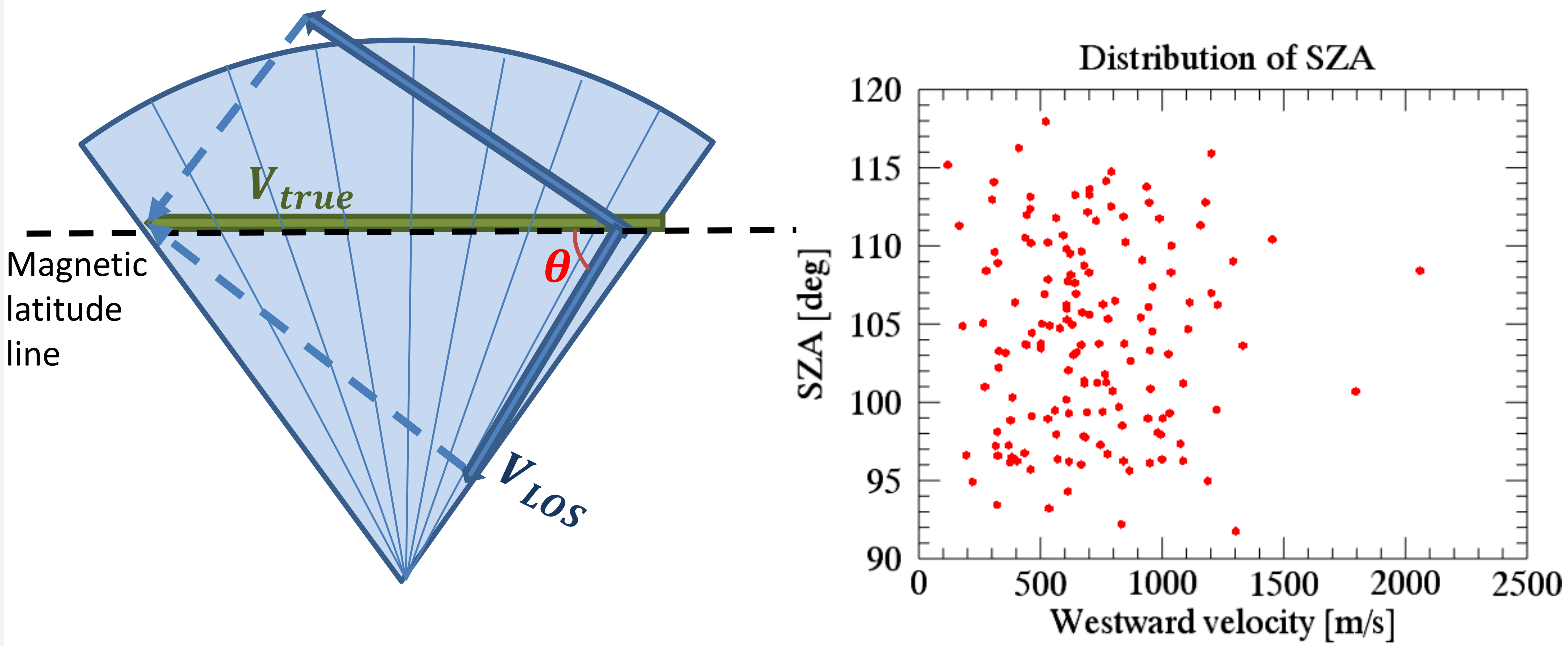

Fig 14. Left figure shows the mechanism of L-shell fitting, while the right figure shows the relation of SZA and westward velocity of SAPS.

1. There are no clear relation between the SAPS velocity and SZA.
2. The lowest velocity of the SAPS events in this study is 180 m/s.

Illuminated height calculated from Chisham model

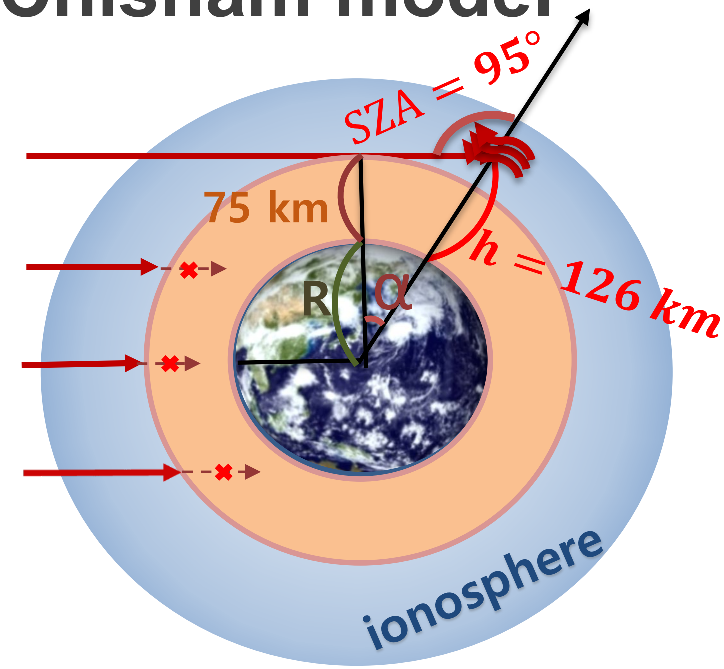

Fig 14. Illuminated atmospheric altitude derived from Chisham model.

- The illuminated height calculated from Chisham model of Hokkaido East radar is 126 km.

- The threshold of illuminated atmospheric altitude for SAPS to generate is just above the peak of Pedersen conductivity.

The altitude distribution of ionospheric Pedersen conductivity

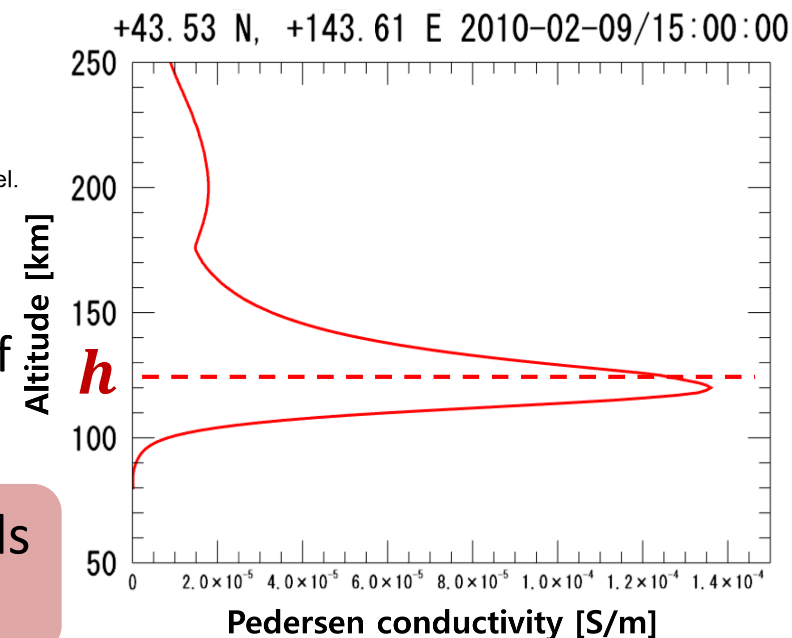

Fig 15. The horizontal and vertical axes show the Pedersen conductivity and the altitude.

Low Pedersen conductivity leads to the generation of SAPS.

Introduction

Motivation & Purpose

Data analysis

Standard model & Chisham model

Results

Conclusions & Future work

Conclusions & Future work

☐ Conclusion

- SAPS tends to appear when the SZA is larger than 95 degrees, and the minimum threshold of illuminated ionospheric altitude is 126 km. This height is just above the peak of Pedersen conductivity, suggesting that Pedersen conductivity is critical for the generation of SAPS.
- The new empirical model of SuperDARN Hokkaido East radar is now being developed. Although it still needs certain adjustments, it is expected to help us achieve more precise estimation of backscatter's geolocation in the future.

☐ Future work

- Detailed investigation of the electric field structure of SAPS by using the electric field data of the Arase satellite.